

## Nuclear Astrophysics at n\_TOF facility, CERN

*G. Tagliente<sup>1</sup>, U. Abbondanno<sup>2</sup>, G. Aerts<sup>3</sup>, H. Alvarez<sup>4</sup>, F. Alvarez-Velarde<sup>5</sup>, S. Andriamonje<sup>3</sup>, J. Andrzejewski<sup>6</sup>, L. Audouin<sup>8</sup>, G. Badurek<sup>9</sup>, P. Baumann<sup>10</sup>, F. Bečvář<sup>11</sup>, F. Belloni<sup>2</sup>, E. Berthoumieux<sup>3</sup>, S. Bisterzo<sup>12</sup>, F. Calviño<sup>13</sup>, M. Calviani<sup>14</sup>, D. Cano-Ott<sup>5</sup>, R. Capote<sup>15,16</sup>, C. Carrapiço<sup>17</sup>, P. Cennini<sup>18</sup>, V. Chepel<sup>19</sup>, E. Chiaveri<sup>18</sup>, N. Colonna<sup>1</sup>, G. Cortes<sup>13</sup>, A. Couture<sup>20</sup>, J. Cox<sup>20</sup>, M. Dahlfors<sup>18</sup>, S. David<sup>10</sup>, I. Dillman<sup>8</sup>, C. Domingo-Pardo<sup>21</sup>, W. Dridi<sup>3</sup>, I. Duran<sup>4</sup>, C. Eleftheriadis<sup>22</sup>, M. Embid-Segura<sup>5</sup>, A. Ferrari<sup>18</sup>, R. Ferreira-Marques<sup>19</sup>, K. Fujii<sup>2</sup>, W. Furman<sup>24</sup>, R. Gallino<sup>12</sup>, I. Goncalves<sup>19</sup>, E. Gonzalez-Romero<sup>5</sup>, F. Gramegna<sup>14</sup>, C. Guerrero<sup>5</sup>, F. Gunsing<sup>3</sup>, B. Haas<sup>25</sup>, R. Haight<sup>26</sup>, M. Heil<sup>8</sup>, A. Herrera-Martinez<sup>18</sup>, M. Igashira<sup>27</sup>, E. Jericha<sup>9</sup>, F. Käppeler<sup>8</sup>, Y. Kadi<sup>18</sup>, D. Karadimos<sup>7</sup>, D. Karamanis<sup>7</sup>, M. Kerveno<sup>10</sup>, P. Koehler<sup>28</sup>, E. Kossionides<sup>29</sup>, M. Krtička<sup>11</sup>, H. Leeb<sup>9</sup>, A. Lindote<sup>19</sup>, I. Lopes<sup>19</sup>, M. Lozano<sup>16</sup>, S. Lukic<sup>10</sup>, J. Marganec<sup>6</sup>, S. Marrone<sup>1</sup>, T. Martinez<sup>5</sup>, C. Massimi<sup>30</sup>, P. Mastinu<sup>14</sup>, A. Mengoni<sup>15</sup>, P. M. Milazzo<sup>2</sup>, M. Mosconi<sup>8</sup>, F. Neves<sup>19</sup>, H. Oberhummer<sup>9</sup>, J. Pancin<sup>3</sup>, C. Papachristodoulou<sup>7</sup>, C. Papadopoulos<sup>31</sup>, C. Paradela<sup>4</sup>, N. Patronis<sup>7</sup>, A. Pavlik<sup>32</sup>, P. Pavlopoulos<sup>33</sup>, L. Perrot<sup>3</sup>, M. T. Pigni<sup>9</sup>, R. Plag<sup>8</sup>, A. Plompen<sup>34</sup>, A. Plukis<sup>3</sup>, A. Poch<sup>13</sup>, J. Praena<sup>14</sup>, C. Pretel<sup>13</sup>, J. Quesada<sup>16</sup>, T. Rauscher<sup>35</sup>, R. Reifarh<sup>26</sup>, C. Rubbia<sup>36</sup>, G. Rudolf<sup>10</sup>, P. Rullhusen<sup>34</sup>, J. Salgado<sup>17</sup>, C. Santos<sup>17</sup>, L. Sarchiapone<sup>18</sup>, I. Savvidis<sup>22</sup>, C. Stephan<sup>23</sup>, J. L. Tain<sup>21</sup>, L. Tassan-Got<sup>23</sup>, L. Tavora<sup>17</sup>, R. Terlizzi<sup>1</sup>, G. Vannini<sup>30</sup>, P. Vaz<sup>17</sup>, A. Ventura<sup>37</sup>, D. Villamarin<sup>5</sup>, M. C. Vincente<sup>5</sup>, V. Vlachoudis<sup>18</sup>, R. Vlastou<sup>31</sup>, F. Voss<sup>8</sup>, S. Walter<sup>8</sup>, H. Wendl<sup>18</sup>, M. Wiescher<sup>20</sup> and K. Wisshak<sup>8</sup>*

<sup>1</sup> INFN, Bari, Italy

<sup>2</sup> INFN, Trieste, Italy

<sup>3</sup> CEA/Irfu, Gif-sur-Yvette, France

<sup>4</sup> Univ. Santiago de Compostela, Spain

<sup>5</sup> CIEMAT, Madrid, Spain

<sup>6</sup> Univ. Lodz, Poland

<sup>7</sup> Univ. Ioannina, Greece

<sup>8</sup> FZK, Institut für Kernphysik, Germany

<sup>9</sup> Technische Universität Wien, Austria

<sup>10</sup> CNRS/IN2P3 - IReS, Strasbourg, France

<sup>11</sup> Univ. Prague, Czech Republic

<sup>12</sup> Dip. Fisica Generale, Univ. Torino, Italy

<sup>13</sup> Univ. Politecnica Catalunya, Barcelona, Spain

<sup>14</sup> INFN, Laboratori Nazionali di Legnaro, Italy

<sup>15</sup> IAEA, Vienna, Austria

<sup>16</sup> Univ. Sevilla, Spain

<sup>17</sup> ITN, Lisbon, Portugal

<sup>18</sup> CERN, Geneva, Switzerland

<sup>19</sup> LIP - Coimbra & Dep. Fisica Univ. Coimbra, Portugal

<sup>20</sup> Univ. Notre Dame, USA

<sup>21</sup> Inst. Fisica Corpuscular, CSIC-Univ. Valencia, Spain

<sup>22</sup> Aristotle Univ. Thessaloniki, Greece

<sup>23</sup> CNR S/IN2P3 - IPN, Orsay, France

<sup>24</sup> JINR, Frank Lab. Neutron Physics, Dubna, Russia

<sup>25</sup> CNRS/IN2P3 - IPN, Orsay, France

<sup>26</sup> LANL, USA

<sup>27</sup> Tokyo Inst. Technology, Japan

<sup>28</sup> ORNL, Physics Division, USA

<sup>29</sup> NCSR, Athens, Greece

<sup>30</sup> Dip. Fisica, Univ. Bologna, & INFN, Bologna, Italy

<sup>31</sup> National Technical Univ. Athens, Greece

<sup>32</sup> Inst. für Fakultät für Physik, Univ. Wien, Austria

<sup>33</sup> Pôle Univ. L. de Vinci, Paris, France<sup>34</sup> CEC-JRC-IRMM, Geel, Belgium<sup>35</sup> Dep. Physics and Astronomy, Univ. Basel, Switzerland<sup>36</sup> Univ. Pavia, Italy<sup>37</sup> ENEA, Bologna, Italy

The n\_TOF Collaboration

**Abstract**

The innovative feature of the n\_TOF facility at CERN, in the two experimental areas, (20 m and 200 m flight paths), allow for an accurate determination of the neutron capture cross section for radioactive samples or for isotopes with small neutron capture cross section, of interest for Nuclear Astrophysics. This contribution presents an overview on the astrophysical program carried on at the n\_TOF facility, the main results and their implications.

**1 Stellar nucleosynthesis**

Elements heavier than Fe are dominantly produced by neutron capture reactions in stars. About half of the elemental abundances are generated in the slow neutron capture process, the s-process, in stellar environments characterized by neutron densities between  $10^6 - 10^{12} \text{ cm}^{-3}$ . In these sites, the nucleosynthesis path proceeds along the stability valley, since  $\beta$ -decays are usually faster than subsequent neutron captures on unstable species. The other half of elemental abundances is produced by the rapid neutron capture process, or r-process. This process is associated with very high neutron densities, higher than  $10^{20} \text{ cm}^{-3}$  and the reaction flow is driven towards the neutron rich side since neutron captures are faster than radioactive decays.

The s-process can be divided in two components called the *main* and the *weak* s-process. The weak component of the s-process, responsible for the a large part of the abundance of isotopes between Fe and Zr, takes place in massive stars ( $M > 15 M_{\odot}$ ) during the He core burning and later during the C shell burning. The main s-process component essentially leads to the production of nuclides between Zr and Bi. It takes place in low mass stars ( $1.5 < M < 3 M_{\odot}$ ) during their asymptotic giant phase.

The nuclear physics inputs for studying the s-process and calculating the s-process abundances are the stellar decay half-lives and the stellar neutron capture cross sections, that is the cross section averaged over the stellar neutron spectrum (Maxwellian Averaged Cross Section, MACS), defined as

$$\langle \sigma \rangle = \frac{2}{\sqrt{\pi}} \frac{1}{(K_B T)^2} \int_0^{\infty} \sigma(E) E \exp\left(-\frac{E}{K_B T}\right) dE \quad (1)$$

where E is the neutron energy,  $K_B$  is the Boltzmann constant and T is the temperature of the stellar site in which the capture process occurs. Since the s-process takes place during different burning stages of the stars the temperature range from 0.1 to 1 GK, corresponding to  $K_B T$  values of 8 to 90 keV. To determine the MACS the excitation function needs to be known up to neutron energies of a few hundred keV.

**2 The n\_TOF facility**

The neutron time-of-flight facility n\_TOF at CERN, based on an idea by Rubbia et al. [1], is a pulsed white neutron source for high-accuracy neutron cross-section measurements over a wide neutron energy range. The neutrons are produced in a monolithic Pb-spallation target, where a pulsed 20 GeV/c proton

beam provided by the CERN Proton Synchrotron (PS) impinges with a maximum repetition rate of 0.8 Hz. The Pb-target is surrounded by an additional moderator layer to generate a neutron beam with energies ranging from thermal up to several GeV. At the facility, operative since 2001, the measurements take place in an experimental area placed at the end of a horizontal beam line, 200 m in length. The experimental conditions and the neutron beam characteristics of this flight path are presented in full detail in Ref. [2].

The horizontal 200 m flight path, with its record instantaneous neutron beam intensity, has allowed very important neutron capture and fission cross-sections measurements, with unprecedented accuracy and energy resolution [3-7]. It has also allowed to extend the energy range to previously unreachable values [8].

In order to extend the experimental possibilities at the n\_TOF facility for cross-section measurements of very low mass sample ( $< 1\text{ mg}$ ), reaction with small cross sections or highly radioactive samples, an additional vertical flight path of 20 m with significantly higher neutron flux was designed and constructed in 2014. The large gain in the neutron flux, of about a factor of 30 relative to the first experimental area, allows one to perform measurements with samples of correspondingly smaller mass or in a shorter time. Most importantly, the combination of the higher flux and shorter time-of-flight, a factor of 10 relative to EAR1, is particularly convenient when measuring radioactive isotopes, as it results in an increase of the signal-to-background ratio of more than two orders of magnitude for the background related to the radioactive decay of the sample. As a consequence, in EAR2 it becomes feasible to perform challenging measurements with isotopes of half-life as short as a few tens of years, offering the unique opportunity to address some open questions in Nuclear Astrophysics.

### 3 Experimental campaign

The n\_TOF Astrophysics experimental campaign is focused on neutron magic nuclei, which act as bottle neck for the flow of s-process, nuclei with  $A < 120$ , branching points isotopes and isotopes of special interest, like the Os isotopes relevant for nuclear cosmochronology.

Of particular interest are the branching points, i.e. radioactive isotopes of relatively short half-life for which a competition exists between neutron capture and the  $\beta$ -decay. The knowledge on the associated cross sections of these isotopes is very poor, mainly due to the difficulty in obtaining enough material and to measure the cross section of sample with a high activity. For these reasons, before 2001 none of these isotopes had been measured yet, despite the fact that they could provide very important information on the thermodynamical conditions of the stellar site in which s-process occurs.

In the following the description and the most recent measurements carried out in the two experimental areas is reported.

#### 3.1 $^{63}\text{Ni}(n,\gamma)$ measurements

The phenomenology of the s-process implies that the solar abundance distribution is composed of two parts: the main component, which mostly accounts for the mass region from Y to Bi, and the weak component, which contributes to the region from the Fe to the Sr. The main and weak component occur prevalently in low mass stars, i.e. with  $1.5M_{\odot} \leq M \leq 3M_{\odot}$  and massive stars with  $M \geq 15M_{\odot}$ . The main difference between these two s-process scenarios is that the high neutron exposure during the main component is sufficient for establishing equilibrium in the reaction flow, resulting in the so-called local approximation, so that the emerging s-abundances are inversely proportional to the stellar cross sections. In this case, the uncertainty on the neutron cross section of an isotope affects only the abundance of that specific isotope. In contrast, the neutron exposure in massive stars is too small to achieve flow equilibrium. As a consequence, the uncertainty in the neutron capture cross section



**Fig. 1:** The s-process reaction path in the Ni-Cu-Zn region during He core burning (dashed lines) and the C shell burning (solid lines) [4]

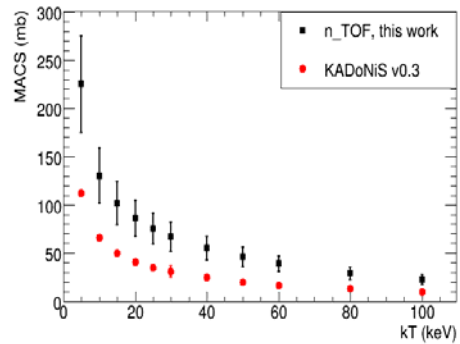


**Fig. 2:** Comparison between the n\_TOF experimental MACS and the theoretical prediction of the KADoNIS compilation

of an isotope not only influences the abundance of that particular isotope but has a potentially strong propagation effect on the abundance of the subsequent isotopes involved in the s-process chain.

The  $^{63}\text{Ni}$  represents the first branching point in the reaction path of the s-process as sketched in Fig.1. In the low neutron density of the weak component, during core He burning the branching is characterized by a significant production of  $^{63}\text{Cu}$  by  $\beta$ -decay from  $^{63}\text{Ni}$ . At much higher neutron density during the C shell burning the branching is closed and the  $^{63}\text{Cu}$  is completely bypassed by the reaction flow. In this phase  $^{63}\text{Cu}$  is only produced by the subsequent decay of the surviving  $^{63}\text{Ni}$  abundance. The neutron capture cross section of  $^{63}\text{Ni}$  is crucial for determining the  $^{63}\text{Cu}/^{65}\text{Cu}$  ratio, which represents a sensitive constraint for stellar model calculations, because the propagation waves of these isotopes affect the entire abundance distribution of the weak s-process [9].

The measurement was performed at n\_TOF with a pair of  $\text{C}_6\text{D}_6$  liquid scintillator detectors. These detectors are optimized to exhibit a very low sensitivity to neutrons, thus minimizing the background produced by neutrons scattered by the sample. Fig. 2 shows the results obtained at n\_TOF in comparison with the KADoNIS compilation [10]. The MACS ranging from  $kT = 5\text{-}100$  keV exhibit total uncertainties of 20-22% and are about a factor 2 higher than the theoretical prediction. These results improved one of the main nuclear uncertainties affecting theoretical predictions for the abundances of  $^{63}\text{Cu}$ ,  $^{64}\text{Ni}$  and  $^{64}\text{Zn}$ .

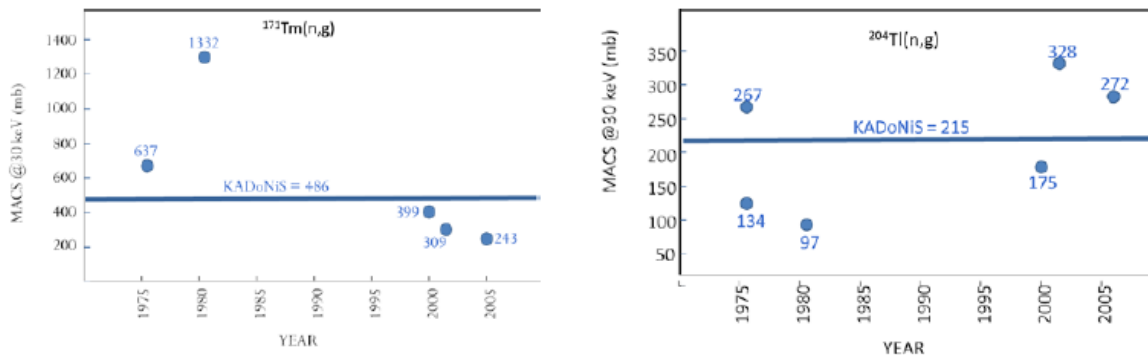


**Fig. 3:** Theoretical prediction of MACS values at 30 keV for  $^{171}\text{Tm}$  and  $^{204}\text{Tl}$

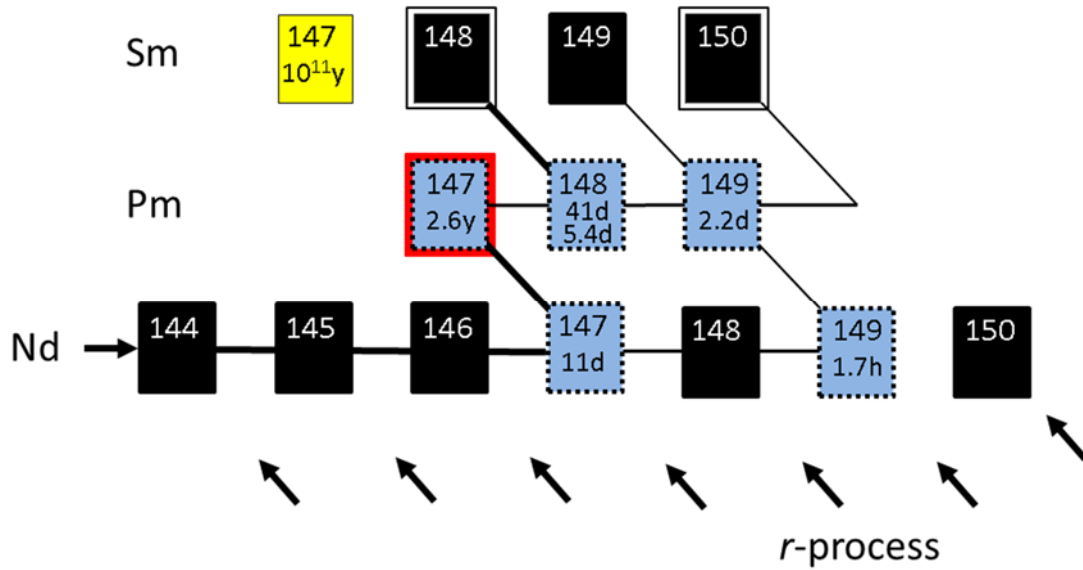


**Fig. 4:** The s-process flow in the mass region  $A=144-150$ . Branching points are indicated by dotted blue boxes.

### 3.2 $^{171}\text{Tm}(n,\gamma)$ and $^{204}\text{Tl}(n,\gamma)$ measurements

The isotopes  $^{171}\text{Tm}$  and the  $^{204}\text{Tl}$  are important s-process branching points [11]. The unstable isotope  $^{171}\text{Tm}$  (half-life of 1.92 years) represents a branching in the s-process path that is independent of stellar temperature and therefore suited to constrain explicitly the s-process neutron density in low mass AGB stars. Being the Tm a rare earth element, the relative abundances of stable isotopes are known with high accuracy.

The isotope  $^{204}\text{Tl}$  (half life of 3.8 years) decays in  $^{204}\text{Pb}$ , which produces  $^{205}\text{Pb}$  when undergoing neutron capture. The fact that both isotopes  $^{204,205}\text{Pb}$  are screened from the r-process by the stable isotopes  $^{204}\text{Hg}$  and  $^{205}\text{Tl}$ , makes  $^{204}\text{Tl}$  particularly interesting; indeed, its capture cross section is of crucial importance for understanding the nucleosynthesis of heavy elements in the AGB stars, but it can also be used to provide chronometric information about the time span between the last s-process nucleosynthesis events that modified the composition of the proto-solar nebula and the formation of solar system solid bodies [12].

At present the values of the neutron capture cross sections of these isotopes used to calculate the abundances in stellar model are based on theoretical predictions. Figure 2 shows the values of the MACS calculated along the years. It is clear that such large uncertainty on the cross section of these isotopes does not allow to make a reliable interpretation of the astrophysical aspect discussed above.

Apart of the natural activity of the samples, which requires a very large instantaneous neutron flux to study their neutron capture cross section, the bigger challenge is to find a sufficient amount of sample material and with enough purity.

To produce the samples of  $^{171}\text{Tm}$  and  $^{204}\text{Tl}$  two pellets of 5 mm diameter of  $^{170}\text{Er}$  (isotopic purity 98,1%) and 225 mg of  $^{203}\text{Tl}$  (isotopic purity 99,5%) have been irradiated with thermal neutron for almost two months at Institute Laue Langevin ILL (Grenoble, France) experimental nuclear reactor.

The irradiation has produced 3.6 mb and 11 mg of  $^{171}\text{Tm}$  and  $^{204}\text{Tl}$ , respectively. After the irradiation, the  $^{204}\text{Tl}$  sample could be directly used for capture measurement because there was not the possibility to separate isotopically the  $^{204}\text{Tl}$  from the initial  $^{203}\text{Tl}$ , while it was possible, using chemical

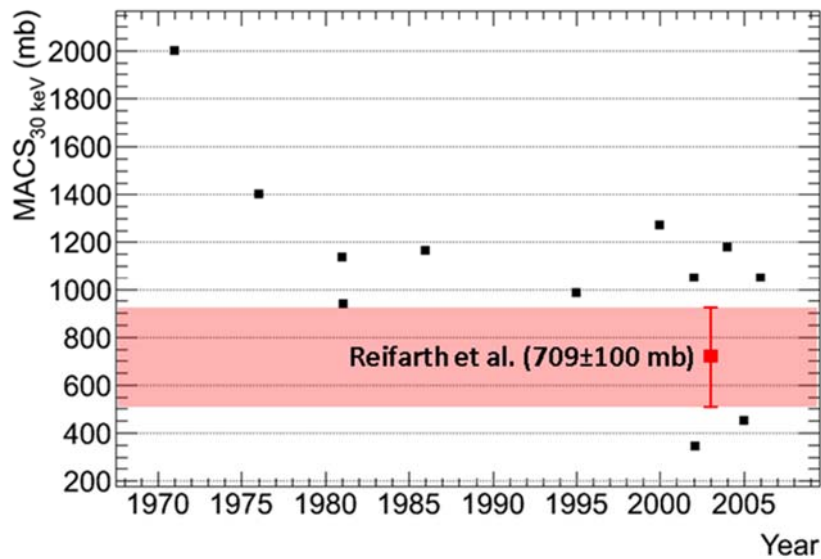


**Fig. 5:** Comparison between the theoretical (black) and experimental (red) MACS values at 30 keV

purification technique, to separate the  $^{171}\text{Tm}$  from the  $^{170}\text{Er}$ . The separation was performed at Paul Scherrer Institute PSI (Villigen, Switzerland).

The measurement had been performed in June 2015 in the EAR1 with a pair of  $\text{C}_6\text{D}_6$  liquid scintillator detectors. The data analysis is currently in progress, but when completed it will provide for the first time experimental information on the capture cross section of these isotopes.

### 3.3 $^{147}\text{Pm}(n,\gamma)$ measurements

The  $^{147}\text{Pm}$  isotope is a branching point in the mass region  $A=147-148$ , that is the Nd-Pm-Sm region. A detailed analysis of this branching is important for modelling the AGB star evolution and to put accurate constraints on the interplay between metallicity and initial stellar mass, mixing processes or hot bottom burning effects [13].

The s-process neutron capture flow in the mass region  $A=144-150$  is reported in Fig. 3, where  $^{148}\text{Sm}$  and  $^{150}\text{Sm}$  are s-only isotopes because they are shielded from the r-process by Nd isotopes. The abundances ratio of  $^{148,150}\text{Sm}$  are well known, being these isotopes rare-earth nuclei, which are not affected by chemical fractionation processes. Therefore this branching can provide very valuable information about the stellar conditions of this process if the capture cross sections of the branching isotopes, mainly  $^{147}\text{Pm}$  but also  $^{147}\text{Nd}$ , are known. Furthermore, the measurement of the  $^{147}\text{Pm}$  capture cross section poses a direct constraint on the stellar reaction rate used in the astrophysical models, since the contribution of neutron capture cross section on thermal populated excited states for  $^{147}\text{Pm}$  are predicted to be very small, between 0% at  $kT=5$  KeV and 6% at  $kT=30$  keV [14,15].

At the present there is only one measurement of the capture cross section of the  $^{147}\text{Pm}$  in the energy region of interest for astrophysics. It is an activation measurement where 28 ng of  $^{147}\text{Pm}$  were irradiated with a Maxwellian neutron energy distribution at  $kT=25$  KeV [16]. As showed in Fig 4 the results are on average 30% smaller than most theoretical predictions.

This result allowed to estimate the range of temperatures and neutron densities in the main s-process component, but it has to be considered that the 95% of neutron exposure in TP-AGB stars

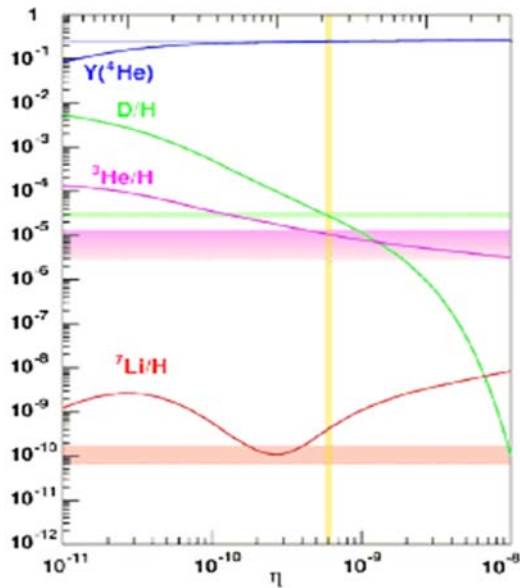


**Fig. 6:** The primordial light element abundances (relative to H) of D,  $^3\text{He}$ ,  $^7\text{Li}$ , and the mass fraction of  $^4\text{He}$  as function of the baryon-to-photon ratio  $\eta$ . The yellow vertical band represents the  $n$  observation from WMAP, while the colored curves and bands respectively.

“Cosmological Lithium problem” [17]. It refers to the large discrepancy between the abundances of primordial  $^7\text{Li}$  predicted by the standard theory of Big Bang Nucleosynthesis (BBN) and the value inferred from the so-called “Spite plateau” in halo stars. The predictions of the BBN theory reproduce successfully the observations of all primordial abundances except for  $^7\text{Li}$ , which is overestimated by more than a factor of 3.

In the standard theory of BBN, 95% of primordial  $^7\text{Li}$  is produced by the decay of  $^7\text{Be}$  ( $t_{1/2}=53.2$  days). Several mechanisms have been put forward to explain the difference between calculations and observation. One possible explanation of the primordial  $^7\text{Li}$  problem is related to the BBN calculations on the production and destruction of  $^7\text{Be}$ . In particular, while the main reaction producing  $^7\text{Be}$ , the  $^3\text{He}(\alpha,\gamma)^7\text{Be}$ , is relatively well known, the cross section for several reactions responsible for its destruction were still uncertain up to recently. To this end several measurements have recently been performed on charge-particle induced reaction on  $^7\text{Be}$ . The results, however, have ruled out the possibility that reaction induced by proton, deuterium or  $^3\text{He}$  could be responsible for the destruction of  $^7\text{Be}$  during the BBN.

In the BBN scenario, neutron-induced reactions on  $^7\text{Be}$  also play a role. However, despite of their importance in the BBN context, very few and uncertain experimental data are available on these reactions. In 1988 the  $^7\text{Be}(n,p)$  was measured at the LANCSE neutron facility, Los Alamos. The result excluded a significant impact of this reaction on the  $^7\text{Li}$  problem [18]. However, because of the limited energy range covered in that measurement, the estimation of the reaction rate at BBN temperature has still to rely on some assumption. Therefore a more precise measurement at temperature between 25-50 keV is needed to improve the reliability of the BBN calculations.

takes place at much lower temperatures of about  $kT = 8$  keV. Therefore, measurement in this energy region was needed.

The sample was produced at ILL irradiating 97 mg of  $^{146}\text{Nd}$  (isotopic purity 98.8%) with thermal neutrons for 56.7 days. This irradiation produced almost 300  $\mu\text{g}$  of  $^{147}\text{Pm}$  via the  $^{146}\text{Nd}(n,\gamma)^{147}\text{Nd}(\beta^-)$  reaction. The Pm was separated from the dominating Nd using the exchange chromatography, precipitation and other radiochemical techniques at the PSI.

The measurement had been performed in July 2015 in EAR2. In fact, due to the small quantity and the high activity of the sample, with its extremely high flux EAR2@n\_TOF is at present the only place where this very challenging time-of-flight measurement could be performed. The experimental setup consisted of four  $\text{C}_6\text{D}_6$  liquid scintillators detectors. In this case as well the data analysis is in progress, but preliminary results indicate that it will be possible to obtain some information on this cross section as well.

### 3.4 $^7\text{Be}(n,\alpha)$ measurement

One of most important unresolved problems of nuclear astrophysics is the so called

The contribution of the  ${}^7\text{Be}(n,\alpha)$  reaction to the destruction of the  ${}^7\text{Be}$  has always been considered negligible in the BBN calculation, due to its much lower estimated cross section. However, this assumption has never been verified experimentally, so that an uncertainty of a factor 10 is typically assigned to this reaction in BBN calculation [19].

One of the main difficulties in the measurement of the  ${}^7\text{Be}(n,\alpha){}^4\text{He}$  cross section is related to the availability of the  ${}^7\text{Be}$  in sufficient quantity and the possibility to handle it. For the measurement at n\_TOF, the sample has been prepared by the Paul Scherrer Institute (PSI), Villigen, with the  ${}^7\text{Be}$  extracted from the cooling of the SINQ spallation source of PSI.

In the  ${}^7\text{Be}(n,\alpha){}^4\text{He}$  reaction, two  $\alpha$ -particles are emitted, back to back, with a relatively high energy of approximately 9 MeV. The  $\alpha$ -particles are detected with a sandwich of two Si-detectors with a sample of  $\sim 2\ \mu\text{g}$  of  ${}^7\text{Bi}$  in between. The two  $\alpha$ -particles are identified on the basis of their relatively high energy and by the coincident method. Two different Si- ${}^7\text{Be}$ -Si sandwiches were prepared at PSI, inserted in a sealed chamber and shipped to CERN. The chamber was then installed on the beam line in EAR2 in late August 2015. Soon afterwards, a 5-weeks long measurement started. Coincidences were clearly observed since the beginning. When completely analysed, this measurement will finally provide, for the first time ever, the cross section as a function of energy. In this case as well, the extremely high neutron flux in EAR2 made possible a measurement that cannot be performed at any other time-of-flight facility in the world.

### 3.5 Conclusion

Neutron capture cross sections of astrophysical interest have been measured at the CERN n\_TOF facility. The major motivation of these measurements is to reduce the uncertainties on nuclear data to a few percent, as required to improve the stellar s-process model.

Since 2014 a second experimental area at 20 m from the spallation target, with a much higher neutron flux is available. This new experimental area now allows measurements of relatively short-lived isotopes, as the s-process branching points, or the (n, charged particle) reactions on  ${}^7\text{Be}$ .

### References

- [1] C. Rubbia *et al.*, Tech. Rep. CERN/LHC/98-02 CERN(1998)
- [2] U. Abbondanno *et al.*, Tech. Rep. CERN/SL/2002-053 ECT(2003)
- [3] U. Abbondanno *et al.*, *Phys. Rev. Letters* **93** (2004)161103
- [4] C. Lederer *et al.*, *Phys. Rev. Letters* **110** (2013) 022501
- [5] F. Gunsing *et al.*, *Phys. Rev. C* **85** (2012)640601
- [6] C. Guerrero *et al.*, *Nuclear Data Sheets*, **119** (2014)5
- [7] M. Calviani *et al.*, *Phys. Rev. C* **85** (2012)34616
- [8] C. Paradela *et al.*, *Phys. Rev. C* **91**(2015) 24602
- [9] M. Heil *et al.*, *Phys. Rev. C* **77**(2008) 015808
- [10] I. Dilmann *et al.*, Proceeding of EFNUDAT Fast Neutrons-Scientific Workshop on Neutron Measurements, Theory & Application, Geel, Belgium, 2009 (Elesvier, Amsterdam, 2006)
- [11] F. Käppeler *et al.*, *Rev. Mod. Phys* **83**(2011)
- [12] K. Yokoi, K. Takahashi and M. Amould, *Astronomy and Astropysics* **145**(1985) 339
- [13] F. Herwig, *Annu. Rev. Astron. Astrophys.* **43**, (2005) 435
- [14] T. Rausher, *The Astrophys. Journal Letters* **755** L10(2012)
- [15] T. Rausher, *The Astrophysical Journal Supplement* **201** (2012)26
- [16] R. Reifarh *et al.*, *The Astrophysicl Journal* **582**, (2003)1251
- [17] R.H. Cyburt *et al.*, *Phys. Rev. D* **69** (2004) 123519
- [18] P.Koehler *et al.*, *Phys. Rev. C* **37**(1988)917
- [19] P.D. Serpico *et al.*, *Jour. Cos. Astropart. Phys.***12**(2994)010